Mode analysis of graded-index optical fibers using a scalar wave equation including gradient-index terms and direct numerical integration

Yasuo Kokubun and Kenichi Iga

Tokyo Institute of Technology, Research Laboratory of Precision Machinery and Electronics, 4259 Nagatsuta, Midoriku, Yokohama, Japan 227

(Received 6 July 1979)

A new mode analysis is proposed for optical fibers with arbitrary refractive-index profile. Scalar wave equations including gradient-index terms and characteristic equations including an abrupt change of the refractive index at the core-cladding boundary are derived for HE, EH, TE, and TM modes. The propagation constant, cutoff frequency, group velocity, and field distribution of each mode are calculated with high accuracy by direct numerical integration of a differential equation and the numerical solution of a transcendental equation.

INTRODUCTION

The optical fiber has merits as an information transmission line for such properties as low loss and wide bandwidth. The mode analysis of optical fibers with arbitrary refractive-index profile is necessary for understanding the transmission characteristics of not only graded-index multimode fibers but also single-mode and dual-mode fibers.[1,2] The field distribution and propagation constant are determined by both the wave equation derived from Maxwell's equations and the characteristic equation derived from the boundary condition at the core-cladding boundary. The wave equation consists of two second-order differential equations coupled to each other owing to the gradient-index term (vector wave equation).[3] These coupled differential equations are difficult to solve analytically and require much time to solve numerically.[4] Thus far, the scalar wave equation, ignoring gradient terms, has been used to describe the field distribution and propagation constant of the fiber. Various approximation methods such as the perturbation method,[5] the WKB method,[6–8] the variational method[9] and the power-series-expansion method[10] were used to solve this equation, but these are not accurate enough to obtain the solution for the single-mode and dual-mode regions. On the other hand, as a vector analysis, the perturbation method,[3] which treats the gradient-index terms as a perturbation, was used for the parabolic-index distribution, and the stratified multilayer matrix method[11] and the finite element method[12] were proposed for an arbitrary graded-index fiber. However, these aim at only the numerical calculation.

On the other hand, if the scalar wave equation including the gradient-index term is derived, conventional approximation methods (such as the variational method, the power-series-expansion method, etc.) can be applied to solve this problem, and it becomes possible to numerically integrate this equation with reduced computation time. However, in the conventional analysis,[13] only the scalar wave equation, ignoring all the gradient-index terms, was obtained as the result of an approximation.

 0030-3941/80/040388-07$00.50

In this paper, (i) scalar wave equations and characteristic equations are derived for a fiber which has a graded index inside the core and an abrupt change of the refractive index at the core-cladding boundary, and (ii) a new mode analysis that utilizes the combination of direct numerical integration of a differential equation and numerical solution of a transcendental equation is proposed. The propagation constant, cutoff frequency, group velocity, and field distribution of HE, EH, TE, and TM modes are calculated by means of this mode analysis.

I. DERIVATION OF SCALAR WAVE EQUATION INCLUDING GRADIENT-INDEX TERMS

In this paper, we consider a cylindrically symmetric fiber and employ the notation of Ref. 13. The arbitrary permittivity distribution is described by

$$\begin{aligned} \epsilon(r) &= \epsilon_1[1-h(r)] && r \leqq a \\ &= \epsilon_2 && r > a, \end{aligned} \tag{1}$$

where a is the core radius, ϵ_2 is the permittivity in the cladding, and ϵ_1 is the maximum value of the permittivity (see Fig. 1). Therefore, $h(r) \geqq 0$. The refractive indices are given by

$$n_1 = \sqrt{\epsilon_1/\epsilon_0}$$

and

$$n_2 = \sqrt{\epsilon_2/\epsilon_0}. \tag{2}$$

The axial field components, E_z and H_z, in cylindrical coordinates are

$$E_z = \frac{\omega^2\epsilon_1\mu_0}{\beta}\Phi(r)e^{j(n\theta+\phi)}, \tag{3}$$

$$H_z = \omega\epsilon_1\Psi(r)e^{j(n\theta+\phi-\pi/2)}, \tag{4}$$

where n is an integer, $\phi = 0$ or $\pi/2$, and $\Phi(r)$ and $\Psi(r)$ are functions of r. In Eqs. (3) and (4), the exponential dependence $e^{j(\omega t-\beta z)}$ on time t and distance z is omitted for simplicity, where ω is the radial frequency and β the propagation constant. By substituting Eqs. (3) and (4) into Maxwell's equations, the following pair of simultaneous differential equations are derived:

$$\begin{aligned} (\chi-h)\frac{1}{r}\frac{d}{dr}\left[\left(\frac{1}{\chi-h}\right)r\frac{d\Phi}{dr}\right] &+ \left[\omega^2\epsilon_1\mu_0(\chi-h) - \frac{n^2}{r^2}\right]\Phi \\ &+ \frac{n}{r}(\chi-h)\frac{d}{dr}\left(\frac{1}{\chi-h}\right)\Psi \\ &+ \frac{1}{(1-h)}\frac{d(1-h)}{dr}\left[\frac{d\Phi}{dr}+\frac{n}{r}\Psi\right] = 0, \end{aligned} \tag{5}$$

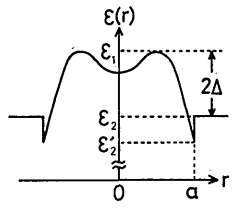

FIG. 1. Cylindrically symmetric dielectric distribution.

$$(\chi-h)\frac{1}{r}\frac{d}{dr}\left[\left(\frac{1}{\chi-h}\right)r\frac{d\Psi}{dr}\right] + \left[\omega^2\epsilon_1\mu_0(\chi-h) - \frac{n^2}{r^2}\right]\Psi + \frac{n}{r}(\chi-h)\frac{d}{dr}\left(\frac{1}{\chi-h}\right)\Phi = 0, \tag{6}$$

where the parameter χ is defined by

$$\chi = 1 - \beta^2/\omega^2\epsilon_1\mu_0. \tag{7}$$

The remaining transverse components E_r, E_θ, H_r, and H_θ are obtained by substituting Eqs. (3) and (4) into Maxwell's equations:

$$E_r = -j\frac{1}{(\chi-h)}\left[\frac{d\Phi}{dr}+\frac{n}{r}\Psi\right]e^{j(n\theta+\phi)}, \tag{8}$$

$$E_\theta = j\frac{1}{(\chi-h)}\left[\frac{d\Psi}{dr}+\frac{n}{r}\Phi\right]e^{j(n\theta+\phi-\pi/2)}, \tag{9}$$

$$H_r = -j\frac{\beta}{\omega\mu_0}\frac{1}{(\chi-h)}\left[\frac{d\Psi}{dr}+\left(\frac{1-h}{1-\chi}\right)\frac{n}{r}\Phi\right]e^{j(n\theta+\phi-\pi/2)}, \tag{10}$$

$$H_\theta = -j\frac{\beta}{\omega\mu_0}\frac{1}{(\chi-h)}\left[\left(\frac{1-h}{1-\chi}\right)\frac{d\Phi}{dr}+\frac{n}{r}\Psi\right]e^{j(n\theta+\phi)}. \tag{11}$$

A. Hybrid modes

First we consider the case $n \neq 0$. Let us define new functions $G_1(r)$ and $G_2(r)$ by

$$G_1(r) = \frac{\Phi(r)+\Psi(r)}{2}, \tag{12}$$

$$G_2(r) = \frac{\Phi(r)-\Psi(r)}{2}. \tag{13}$$

Addition and subtraction of Eqs. (5) and (6) give

$$\begin{aligned} (\chi-h)\frac{1}{r}\frac{d}{dr}\left[\left(\frac{1}{\chi-h}\right)r\frac{dG_1}{dr}\right] &+ \left[\omega^2\epsilon_1\mu_0(\chi-h) - \frac{n^2}{r^2}\right]G_1 + \frac{n}{r}(\chi-h)\frac{d}{dr}\left(\frac{1}{\chi-h}\right)G_1 \\ &+ \frac{1}{2}\frac{1}{(1-h)}\frac{d(1-h)}{dr}\left[\frac{d(G_1+G_2)}{dr}+\frac{n}{r}(G_1+G_2)\right] = 0, \end{aligned} \tag{14}$$

$$\begin{aligned} (\chi-h)\frac{1}{r}\frac{d}{dr}\left[\left(\frac{1}{\chi-h}\right)r\frac{dG_2}{dr}\right] &+ \left[\omega^2\epsilon_1\mu_0(\chi-h) - \frac{n^2}{r^2}\right]G_2 - \frac{n}{r}(\chi-h)\frac{d}{dr}\left(\frac{1}{\chi-h}\right)G_2 \\ &+ \frac{1}{2}\frac{1}{(1-h)}\frac{d(1-h)}{dr}\left[\frac{d(G_1+G_2)}{dr}+\frac{n}{r}(G_1+G_2)\right] = 0, \end{aligned} \tag{15}$$

TABLE I. Values of parameter P in the case of a step-index profile.

	Far from cutoff	At cutoff
HE	−1	−1
EH	+1	ϵ_1/ϵ_2 ($\cong$ +1)

respectively. These two equations couple to each other owing to the gradient term. If we neglect this coupling, Eqs. (14) and (15) reduce to two independent differential equations, and each of them gives the scalar wave equation for the HE and EH modes, respectively.[13] However, if we examine the gradient term more carefully, we see that a small part of it contributes the coupling between Eqs. (14) and (15). This can be explained in the following way.

According to Ref. (14), the parameter P, which is defined by

$$P = \frac{\omega\mu_0}{\beta}\frac{jH_z}{E_z} = \frac{\Psi}{\Phi} = \frac{G_1 - G_2}{G_1 + G_2}, \tag{16}$$

is approximated to be ± 1 for the step-index fiber as shown in Table I. Since this approximation is expected to hold for graded-index fibers with an appropriate accuracy, either G_1 or G_2 is also approximated to be zero.[11] Therefore, Eqs. (14) and (15) become two independent differential equations, and they include the gradient term.[15] The case with $G_1 \neq 0$ and $G_2 = 0$ ($\Phi = \Psi = G_1$) corresponds to HE modes, and the case with $G_1 = 0$ and $G_2 \neq 0$ ($\Phi = -\Psi = G_2$) corresponds to EH modes.

For HE modes, we introduce a new scalar wave function

$$R(r) = -j\frac{(1-h)^{1/2}}{(\chi - h)}\left[\frac{dG_1}{dr} + \frac{n}{r}G_1\right]. \tag{17}$$

Assuming $G_2 = 0$, substitution of Eq. (17) into (14) gives

$$G_1(r) = -j\frac{1}{\omega^2\epsilon_1\mu_0(1-h)^{1/2}}\left[\frac{dR}{dr} - \frac{n-1}{r}R\right]. \tag{18}$$

Further, substitution of Eq. (18) into (17) yields the following scalar wave equation:

$$\frac{1}{r}\frac{d}{dr}\left[r\frac{dR}{dr}\right] + \left[\omega^2\epsilon_1\mu_0(\chi - h) - \frac{(n-1)^2}{r^2}\right]R - \frac{1}{2}\frac{1}{(1-h)}\frac{d(1-h)}{dr}\left[\frac{dR}{dr} - \frac{n-1}{r}R\right] = 0. \tag{19}$$

Rewriting the dielectric distribution function $h(r)$ as

$$h(\rho) = 2\Delta f(\rho), \tag{20}$$

where $\rho = r/a$ and $2\Delta = (\epsilon_1 - \epsilon_2)/\epsilon_1$, and defining new parameters b and V by

$$b = \frac{(\beta/k_0)^2 - n_2^2}{n_1^2 - n_2^2}, \tag{21}$$

$$V = k_0 n_1 a\sqrt{2\Delta} \qquad (k_0 = 2\pi/\lambda), \tag{22}$$

Eq. (19) can be rewritten as in Table II. It is interesting to note that Eq. (19) includes gradient terms although it is a scalar wave equation.

As for EH modes, upon defining a new scalar wave function $R(r)$ by

$$R(r) = -j\frac{(1-h)^{1/2}}{(\chi - h)}\left[\frac{dG_2}{dr} - \frac{n}{r}G_2\right], \tag{23}$$

the scalar wave equation is derived in the same manner and the result is shown in Table II.

In order to describe the transverse field components simply, we introduce circularly polarized components[11] defined by

$$E^{\pm} = E_r \pm jE_\theta, \tag{24}$$

$$H^{\pm} = H_r \pm jH_\theta, \tag{25}$$

$$F_z^{\pm} = jE_z \pm (\omega\mu_0/\beta)H_z. \tag{26}$$

By using Eqs. (3), (4), and (8)–(11), Eqs. (24)–(26) become

$$E^{\pm} = -j\frac{1}{(\chi - h)}\left[\frac{d(\Phi \mp \Psi)}{dr} \mp \frac{n}{r}(\Phi \mp \Psi)\right], \tag{27}$$

$$H^{\pm} = -\frac{\beta}{\omega\mu_0}\frac{1}{(\chi - h)}\left[\left(\frac{d\Psi}{dr} \mp \frac{n}{r}\Psi\right) \pm \left(\frac{1-h}{1-\chi}\right)\left(\frac{d\Phi}{dr} \mp \frac{n}{r}\Phi\right)\right], \tag{28}$$

TABLE II. Scalar wave equation including gradient terms and relationships among Φ, Ψ, and R.

Mode	Scalar wave equation	Relationships among Φ, Ψ, and R
HE	$\frac{1}{\rho}\frac{d}{d\rho}\left(\rho\frac{dR}{d\rho}\right) + \left\{V^2[1-b-f(\rho)] - \frac{(n\mp 1)^2}{\rho^2}\right\}R + \frac{1}{2}\frac{2\Delta}{(1-2\Delta f(\rho))}\frac{df}{d\rho}\left[\frac{dR}{d\rho} \mp \frac{(n\mp 1)}{\rho}R\right] = 0$	$\Phi = \Psi = -j\frac{1}{\omega^2\epsilon_1\mu_0 a[1-2\Delta f(\rho)]^{1/2}}\left[\frac{dR}{d\rho} - \frac{n-1}{\rho}R\right]$
EH	−: HE mode +: EH mode	$\Phi = -\Psi = -j\frac{1}{\omega^2\epsilon_1\mu_0 a[1-2\Delta f(\rho)]^{1/2}}\left[\frac{dR}{d\rho} + \frac{n+1}{\rho}R\right]$
TE	$\frac{1}{\rho}\frac{d}{d\rho}\left(\rho\frac{dR}{d\rho}\right) + \left\{V^2[1-b-f(\rho)] - \frac{1}{\rho^2}\right\}R = 0$	$\Phi = 0, \quad \Psi = j\frac{1}{\omega^2\epsilon_1\mu_0 a}\left[\frac{dR}{d\rho} + \frac{1}{\rho}R\right]$
TM	$\frac{1}{\rho}\frac{d}{d\rho}\left(\rho\frac{dR}{d\rho}\right) + \left\{V^2[1-b-f(\rho)] - \frac{1}{\rho^2}\right\}R + \frac{2\Delta}{1-2\Delta f(\rho)}\frac{df}{d\rho}\left[\frac{dR}{d\rho} + \frac{1}{\rho}R\right] = 0$	$\Psi = 0, \quad \Phi = -j\frac{1}{\omega^2\epsilon_1\mu_0 a[1-2\Delta f(\rho)]}\left[\frac{dR}{d\rho} + \frac{1}{\rho}R\right]$

$$F_z^{\pm} = j\frac{\omega^2\epsilon_1\mu_0}{\beta}(\Phi \pm \Psi)e^{j(n\theta+\phi)}. \quad (29)$$

By substituting the relationships among Φ, ψ, and R into Eqs. (27)–(29), it can easily be seen that the plus components become zero for HE modes and the minus components become zero for EH modes. The results are summarized in Table III.

B. TE and TM modes

When $n = 0$, Eqs. (5) and (6) become two independent differential equations. The case with $\Phi = 0$ and $\psi \neq 0$ corresponds to TE modes, and the case $\Phi \neq 0$ and $\psi = 0$ corresponds to TM modes.

For TM modes, we define the scalar wave function $R(r)$ by

$$R(r) = j\left(\frac{1-h}{\chi-h}\right)\frac{d\Phi}{dr}. \quad (30)$$

Substitution of Eq. (30) into Eq. (5) yields

$$\Phi(r) = j\frac{1}{\omega^2\epsilon_1\mu_0(1-h)}\left[\frac{dR}{dr}+\frac{1}{r}R\right]. \quad (31)$$

The scalar wave equation is obtained by substituting Eq. (31) into Eq. (30) as follows

$$\frac{1}{r}\frac{d}{dr}\left[r\frac{dR}{dr}\right] + \left[\omega^2\epsilon_1\mu_0(\chi-h) - \frac{1}{r^2}\right]R - \frac{1}{(1-h)}\frac{d(1-h)}{dr}\left[\frac{dR}{dr}+\frac{1}{r}R\right] = 0. \quad (32)$$

Further, Eq. (32) is rewritten as shown in Table II by using Eqs. (20)–(22). Eq. (32) also includes the gradient term, although the approximation such as $P = \pm 1$ which was used for hybrid modes is not used at all.

The transverse components are given by using Eqs. (8)–(11) and (31) as

$$E_r = \frac{1}{(1-h)}R(r)e^{j(n\theta+\phi)}, \quad (33)$$

$$H_\theta = \frac{\beta}{\omega\mu_0}\frac{1}{(1-\chi)}R(r)e^{j(n\theta+\phi)}, \quad (34)$$

$$E_\theta = H_r = 0. \quad (35)$$

As for TE modes, defining the scalar wave function by

$$R(r) = -j\frac{1}{(\chi-h)}\frac{d\Psi}{dr}, \quad (36)$$

we derive the scalar wave equation in the same manner and the result is shown in Table II. This equation does not include the gradient term.

The transverse field components are given by

$$E_\theta = R(r)e^{j(n\theta+\phi)}, \quad (37)$$

TABLE III. Transverse field component of each mode.

Mode	Transverse field component
HE	$E^- = \frac{2}{(1-h)^{1/2}}R(\rho)e^{j(n\theta+\phi)}$
	$H^- = j\frac{\beta}{\omega\mu_0}\frac{1}{(1-h)^{1/2}}\left[\frac{1-h}{1-\chi}+1\right]R(\rho)e^{j(n\theta+\phi)}$
	$E^+ = 0, \quad H^+ \cong 0$
EH	$E^+ = \frac{2}{(1-h)^{1/2}}R(\rho)e^{j(n\theta+\phi)}$
	$H^+ = j\frac{\beta}{\omega\mu_0}\frac{1}{(1-h)^{1/2}}\left[\frac{1-h}{1-\chi}+1\right]R(\rho)e^{j(n\theta+\phi)}$
	$E^- = 0, \quad H^- \cong 0$
TE	$E_\theta = R(\rho)e^{j(n\theta+\phi)}$
	$H_r = -\frac{\beta}{\omega\mu_0}R(\rho)e^{j(n\theta+\phi)}$
	$E_z = E_r = H_\theta = 0$
TM	$E_r = \frac{1}{(1-h)}R(\rho)e^{j(n\theta+\phi)}$
	$H_\theta = \frac{\beta}{\omega\mu_0}\frac{1}{(1-\chi)}R(\rho)e^{j(n\theta+\phi)}$
	$H_z = E_\theta = H_r = 0$

$$H_r = -(\beta/\omega\mu_0)R(r)e^{j(n\theta+\phi)}, \quad (38)$$

$$E_r = H_\theta = 0. \quad (39)$$

II. CHARACTERISTIC EQUATION

A. Hybrid modes

In the case with $n \neq 0$, the assumption that $P = \pm 1$ implies that circularly polarized components with one sign (plus or minus) defined by Eqs. (24)–(26) are zero. The boundary condition for these circular polarized components is given by[11]

$$\begin{bmatrix} F_z^{\pm} \\ E^{\pm} \end{bmatrix}_{r=a+0} = \begin{bmatrix} 1 & 0 \\ 0 & \frac{\epsilon_2+\epsilon_2'}{2\epsilon_2} \end{bmatrix}\begin{bmatrix} F_z^{\pm} \\ E^{\pm} \end{bmatrix}_{r=a-0}, \quad (40)$$

where ϵ_2 is the dielectric constant in the cladding and $\epsilon_2' = \epsilon_1[1 - 2\Delta f(1)]$. The scalar wave function $R(\rho)$ in the cladding is expressed by the modified Bessel function of the second kind as

$$R(\rho) = AK_m(w\rho), \quad (41)$$

where A is a constant, $w = \sqrt{\beta^2 - k_0^2 n_2^2}\, a$, and

TABLE IV. Characteristic equation and cutoff condition of each mode.

Mode	Characteristic equation	Cutoff condition
HE	$\left[\frac{1}{R(\rho)}\frac{dR(\rho)}{d\rho}\Big\|_{\rho=1} - (n-1)\right] = \frac{\epsilon_2+\epsilon_2'}{2\epsilon_2}\left[-\frac{wK_n(w)}{K_{n-1}(w)}\right]$	$\frac{1}{R(\rho)}\frac{dR(\rho)}{d\rho}\Big\|_{\rho=1} + \frac{\epsilon_2'}{\epsilon_2}(n-1) = 0$
EH	$\left[\frac{1}{R(\rho)}\frac{dR(\rho)}{d\rho}\Big\|_{\rho=1} + (n+1)\right] = \frac{\epsilon_2+\epsilon_2'}{2\epsilon_2}\left[-\frac{wK_n(w)}{K_{n+1}(w)}\right]$	$\frac{1}{R(\rho)}\frac{dR(\rho)}{d\rho}\Big\|_{\rho=1} + (n+1) = 0$
TE	$\frac{1}{R(\rho)}\frac{dR(\rho)}{d\rho}\Big\|_{\rho=1} = -\frac{wK_0(w)}{K_1(w)} - 1$	$\frac{1}{R(\rho)}\frac{dR(\rho)}{d\rho}\Big\|_{\rho=1} + 1 = 0$
TM	$\left[\frac{1}{R(\rho)}\frac{dR(\rho)}{d\rho}\Big\|_{\rho=1} + 1\right] = \frac{\epsilon_2}{\epsilon_2'}\left[-\frac{wK_0(w)}{K_1(w)}\right]$	$\frac{1}{R(\rho)}\frac{dR(\rho)}{d\rho}\Big\|_{\rho=1} + 1 = 0$

$$m = \begin{cases} n-1\text{: HE mode} \\ n+1\text{: EH mode} \\ 1\text{: TE and TM modes.} \end{cases} \quad (42)$$

The characteristic equation is then derived as shown in Table IV by using Eqs. (27), (29), (40), (41) and the relationships among Φ, Ψ, and R given in Table II.

B. TE and TM modes

In the case with $n = 0$, the characteristic equations for TE and TM modes are derived as shown in Table IV from the boundary conditions that the tangential field components E_z, E_θ, H_z and H_θ are continuous at the core-cladding boundary, instead of considering the circularly polarized components.

C. Cutoff conditions

At cutoff, the propagation constant β approaches $k_0 n_2$, and so w reaches zero. The cutoff condition can be obtained from the characteristic equations by using the asymptotic formulas of the modified Bessel functions at the limit of $w \to 0$. The results are summarized in Table IV together with the characteristic equations.

III. NUMERICAL CALCULATION

The propagation constant of graded-index fibers is determined from the condition that two field functions, namely, one in the core and the other in the cladding, satisfy independently the scalar wave function given in Table II and that these fields satisfy the characteristic equation given in Table IV simultaneously. In this paper, the scalar wave equation is solved numerically by means of a direct integration method (Milne method) and the characteristic equation is solved by means of the numerical solution of a transcendental equation. The propagation constant, cutoff frequency, group velocity, and field distribution of each mode are calculated by using these two numerical solutions simultaneously.

A. Steps of numerical calculation

1. Propagation constant

(i) First, we suppose that the normalized propagation constant b is given a certain value (for example, $b = 0$). The normalized frequency V is fixed to be a required value.

(ii) In the vicinity of $\rho = 0$, the scalar wave function $R(\rho)$ is approximated to be

$$R(\rho) = AJ_{n\pm1}(u_0\rho), \quad (43)$$

where A is a constant, $J_m(x)$ is the Bessel function of mth order, and $u_0 = \sqrt{k_0^2 n^2(0) - \beta^2}\, a$. The plus sign corresponds to the EH mode, the minus sign to the HE mode, and $n = 0$ corresponds to the TE and TM modes.

(iii) The scalar wave equation is solved by means of the direct integration method (Milne method) under the initial condition of Eq. (43), and the values of $R(\rho)$ and $dR(\rho)/d\rho$ at $\rho = 1$ are obtained.

(iv) Let us define a new function $I(V,b)$ by

$I(V,b)$ = (left-hand side of the characteristic equation)

− (right-hand side of the characteristic equation).

Since the values of V and b are given at step (i), the value of $I(V,b)$ can be calculated by using the values of $R(\rho)$ and $dR(\rho)/d\rho$ at $\rho = 1$ obtained in step (iii).

(v) Determine whether the value of $I(V,b)$ is close enough to zero or not. If the value is not close to zero, the

TABLE V. Cutoff frequency of each mode in a parabolic-index fiber [comparison of values in Ref. (16)].

LP	Analytical solution[16]	Stratified multilayer method[18]	This analysis ($\Delta = 0.5\%$)	HE, EH, TE, TM
1,1	3.518	3.517	3.521 16	HE_{21}
			3.517 52	TE_{01}
			3.513 37	TM_{01}
0,2	5.068	5.061	5.066 24	HE_{12}
2,1	5.744	5.747	5.746 26	HE_{31}
			5.740 36	EH_{11}
1,2	7.451	7.448	7.451 68	HE_{22}
			7.450 37	TE_{02}
			7.447 59	TM_{02}

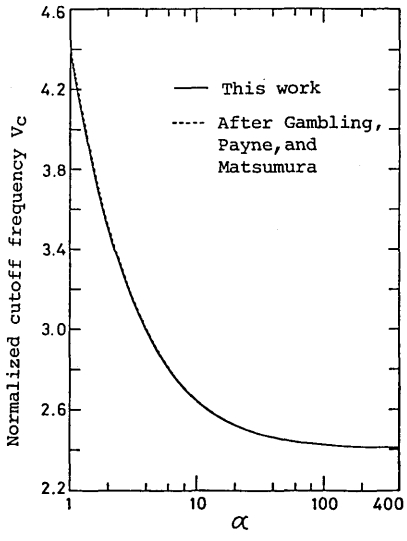

FIG. 2. Cutoff frequency of TE_{01} mode of α-power-law fibers.

initial value of b given at step (i) is then revised and the above steps repeated until the value converges to zero.

(vi) The propagation constant is obtained from the value of b when the value of $I(V,b)$ converges to zero.

2. Cutoff frequency

In the above step (i), the roles of b and V are exchanged (b is fixed to be zero), and the above steps are repeated with respect to V. The cutoff frequency is the V value at the time of convergence of $I(V,b)$ to zero.

3. Group velocity

After $I(V,b)$ converges to zero, the group velocity is calculated by

$$\frac{db}{dV} = -\frac{\partial I(V,b)/\partial V}{\partial I(V,b)/\partial b} \simeq -\frac{I(V+\delta,b)}{I(V,b+\delta)}, \tag{44}$$

$$v_g = C\frac{[n_2^2 + (n_1^2 - n_2^2)b]^{1/2}}{n_2N_2 + [b + (1/2)V(db/dV)](n_1N_1 - n_2N_2)}, \tag{45}$$

where δ is an arbitrary small number, C is the velocity of light in a vacuum, and

$$N_1 = \frac{d(kn_1)}{dk}$$

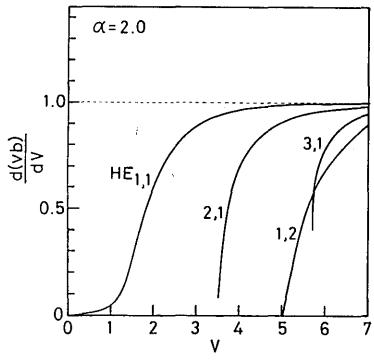

FIG. 3. Group delay characteristic of parabolic-index profile.

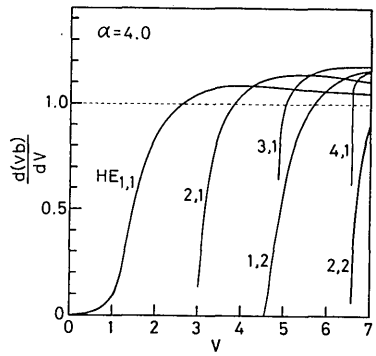

FIG. 4. Group delay characteristic of fourth-power-law index profile.

and

$$N_2 = \frac{d(kn_2)}{dk}. \tag{46}$$

4. Field distribution

The field distribution can be calculated by substituting $R(\rho)$ obtained at step (iii) into Eqs. (27)–(29) for hybrid modes, into Eqs. (33)–(35) for TM modes, and into Eqs. (37)–(39) for TE modes, respectively.

B. Numerical results

In order to confirm the accuracy of this analysis, the cutoff frequency of a parabolic-index profile was calculated and compared with the result of Ref. (16) (see Table V). When the number of divided points in the numerical integration was 9000, the error in the cutoff frequency of the TE_{01} mode was within 0.01%. In this analysis, the degeneracy of LP modes is removed because of the gradient term in the scalar wave equation. In the case of a parabolic-index profile, the cutoff frequency of the TM_{01} mode is smaller than that of the TE_{01} mode, and the relationship between them can be expressed by

$$V_c = 3.5175 - 8.33 \times 10^{-3}\Delta. \tag{47}$$

Next, the cutoff frequency of the TE_{01} mode of α-power-law profiles is shown in Fig. 2. The number of divided points of numerical integration was 2000, and the result of this analysis (solid curve) coincides with that of Ref. (17) (dashed curve) within an error of 0.1%. Lastly, the group delay characteristics of parabolic, fourth power, and tenth power index profiles are shown in Figs. 3, 4, and 5, respectively.

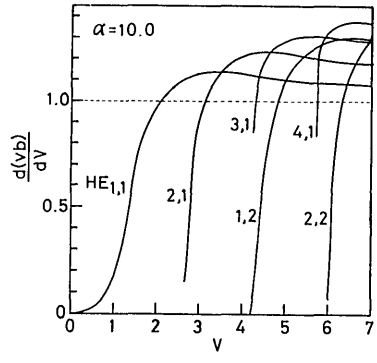

FIG. 5. Group delay characteristic of tenth-power-law index profile.

IV. CONCLUSION

The scalar wave equation including the gradient-index term and the characteristic equation including an abrupt change of the refractive index at the core-cladding boundary was derived for each of the HE, EH, TE, and TM modes, and a new numerical solution combining direct integration of the differential equation with numerical solution of the transcendental equation was investigated. In this analysis, the degeneracies in propagation constant, group velocity, cutoff frequency, and field distribution of LP modes are removed, because the scalar wave equation includes most of the gradient-index term and the characteristic equation includes an abrupt change of the refractive index at the core-cladding boundary.

Thus this analysis seems to correspond to the 2×2 matrix analysis of the stratified multilayer matrix method,[11] because the parameter P defined by Eq. (16) is approximated to be ± 1. The computation time required to obtain the same amount of accuracy is almost the same. The stratified multilayer matrix method includes the gradient-index term as the boundary condition at each boundary between adjacent layers. On the other hand, this analysis includes the gradient-index term in the scalar wave equation and the field distribution is obtained by means of direct numerical integration.

ACKNOWLEDGMENTS

The authors express their sincere thanks to Professor Y. Suematsu, Associate Professor Y. Naito, and Associate Professor K. Furuya for their valuable discussions on this work, and to Dr. C. Lin, Bell Laboratories, for comments on this paper.

[1]J. Sakai and T. Kimura, "Large-core broadband optical fiber," Opt. Lett. **1**, 169–171 (1977).

[2]K. Iga and Y. Kokubun, "A design and experiment for group-delay-difference-free dual mode optical fibers," TGOQE, IECE Jpn, No. OQE78-36 (1978).

[3]Y. Suematsu and K. Furuya, "Vector wave solution of light beam propagating along lens-like medium," J. IECE Jpn **54-B**, 325–333 (1971).

[4]G. L. Yip and Y. H. Ahmew, "Propagation characteristics of radially inhomogeneous optical fibre," Electron. Lett. **10**, 37–38 (1974).

[5]Y. Suematsu and K. Iga, "Mode conversion in lightbeam waveguide," J. IECE Jpn **49**, 1645–1652 (1966).

[6]W. Streifer and C. N. Kurtz, "Scalar analysis of radially inhomogeneous guiding media," J. Opt. Soc. Am. **57**, 779–786 (1967).

[7]S. Kawakami and J. Nishizawa, "Kinetics of an optical wave packet in a lens-like medium," J. Appl. Phys. **38**, 4807–4811 (1967).

[8]D. Gloge and E. A. J. Marcatili, "Multimode theory of graded core fibers," Bell Syst. Tech. J. **52**, 1563–1578 (1973).

[9]T. Okoshi and K. Okamoto, "Analysis of wave propagation in inhomogeneous optical fibers using a variational method," IEEE Trans. Microwave Theory Tech., **MTT-22**, 938–945 (1974).

[10]H. Kirchhoff, "Wave propagation along radially inhomogeneous glass fibers," A.E.Ü. **27**, 13–18 (1973).

[11]T. Tanaka and Y. Suematsu, "An exact analysis of cylindrical fiber with index distribution by matrix method and its application to focusing fiber," Trans. IECE Jpn **E59**, 1–8 (1976).

[12]K. Okamoto and T. Okoshi, "Vectorial wave analysis of inhomogeneous optical fibers using finite element method," IEEE Trans. Microwave Theory Tech. **MTT-26**, 109–114 (1978).

[13]C. N. Kurtz and W. Streifer, "Guided waves in inhomogeneous focusing media Part I: Formulation, Solution for quadratic inhomogeneity," IEEE Trans. Microwave Theory Tech. **MTT-17**, 11–15 (1969).

[14]E. Snitzer, "Cylindrical dielectric waveguide modes," J. Opt. Soc. Am. **51**, 491–498 (1961).

[15]Strictly speaking, one of G_1 and G_2 is smaller than the other by a factor of the order of magnitude of Δ. Therefore, even if the coupling terms in Eqs. (14) and (15) are ignored, effective gradient terms [i.e. $(1 - \Delta)$ (gradε)] still remain.

[16]T. I. Lukowski and F. P. Kapron, "Parabolic fiber cutoffs: A comparison of theories," J. Opt. Soc. Am. **67**, 1185–1187 (1977).

[17]W. A. Gambling, D. N. Payne, and H. Matsumura, "Cutoff frequency in radially inhomogeneous single-mode fibre," Electron. Lett. **13**, 139–140 (1977).

[18]E. Bianciardi and V. Rizzili, "Propagation in graded-core fibers: A unified numerical description," Opt. Quantum Electron **9**, 121–123 (1977).